# Identification of Damage in IR-Structures from Earthquake Records - Optimal Location of Sensors

Nielsen, Søren R.K.; Skjærbæk, P. S.; Cakmak, A. S.

*Publication date:*
1996

*Document Version*
Early version, also known as pre-print

INSTITUTTET FOR BYGNINGSTEKNIK
DEPT. OF BUILDING TECHNOLOGY AND STRUCTURAL ENGINEERING
AALBORG UNIVERSITET • AUC • AALBORG • DANMARK

FRACTURE & DYNAMICS
PAPER NO. 77

Submitted to Journal of Soil Dynamics and Structural Engineering

P. S. SKJÆRBÆK, S. R. K. NIELSEN, A. Ş. ÇAKMAK
IDENTIFICATION OF DAMAGE IN RC-STRUCTURES FROM EARTHQUAKE RECORDS - OPTIMAL LOCATION OF SENSORS
APRIL 1996 ISSN 1395-7953 R9614

# Identification of Damage in RC-Structures from Earthquake Records - Optimal Location of Sensors

P.S. Skjærbæk, S.R.K. Nielsen

*Department of Building Technology and Structural Engineering, Aalborg University, DK-9000 Aalborg, Denmark*

and

A.S. Çakmak

*Department of Civil Engineering and Operations Research, Princeton University, Princeton, NJ 08544, USA*

## Abstract

A method for localization of structural damage in seismically excited RC-structures using measured acceleration response time series is presented. From measured response of some or all storeys, the two lowest smoothed eigenfrequencies and mode shape coordinates are estimated. These estimated values are used as input to a developed substructure iteration method where local storey damages are estimated in such a way that these smoothed values are reproduced. The local damage indicator of a substructure is defined as the average reduction of the stiffness matrix of the initial undamaged substructure. The method is applied to simulated data of a 6-storey, 2-bay test frame (scale 1:5) that is to be tested at the Structural Laboratory of Aalborg University, Denmark. The simulations are performed using the non-linear finite element program SARCOF. Special emphasis is put on the investigation of the optimal location of measurement sensors, i.e. at which locations along the structure the most information about the damage distribution is gained. In all cases it is assumed that measurements are performed at top storey and ground surface, and the investigations are concentrated on putting one or two more measurement points in between. The two cases where the structure is excited in the first and second mode are investigated and it is found that in general the sensors should be placed in the lower part of the structure. Furthermore, it is found that the method provides good results even when only the measurements at top storey and ground surface are used.

**Key words:** Damage, Localization, Optimal Sensor Location, Earthquakes, Finite Element Model, Substructures.

## 1 Introduction

When civil engineering structures are subjected to sufficiently high dynamic loads it is well known that some kind of damage will occur somewhere in the structure. In RC-structures the damage may start as cracking developing into crushing of concrete and yielding of reinforcement. The damage may be highly localized or more spread out in the structure. During an earthquake both types of damage may develop in the structure and there is a need for methods to assess the damage in the structure. The traditional way of assessing damage in RC-structures is by visual inspection of the structure by measuring cracks, permanent deformations, etc. This is

The FRACTURE AND DYNAMICS papers are issued for early dissemination of research results from the Structural Fracture and Dynamics Group at the Department of Building Technology and Structural Engineering, University of Aalborg. These papers are generally submitted to scientific meetings, conferences or journals and should therefore not be widely distributed. Whenever possible reference should be given to the final publications (proceedings, journals, etc.) and not to the Fracture and Dynamics papers.

Printed at Aalborg University

often very cumbersome, since panels and other walls covering beams and columns need to be removed. Furthermore, internal damage such as bond slippage can be very difficult to determine by visual inspection. The aim of this paper is therefore to test and improve a method capable of assessing both localized damage and damage spread out in the structure by using storey acceleration measurements during the earthquake only. The quality of the damage assessment is investigated by considering different cases where measurements at one or more storeys are performed.

# 2 Measurement Procedure

During a severe excitation such as a strong motion earthquake, the structure will be sequentially damaged due to cracking, debonding, crushing of concrete and post-yielding of reinforcement bars. The circular eigenfrequencies, $\omega_i(t)$ and mode shapes $\mathbf{\Phi}_i(t)$, of the time-varying structure will vary rapidly as the structure enters and leaves the plastic regime. To extract the long-term tendency of this quantity, which displays the time-variation of the structural parameters due to damages, a smoothing, denoted $\langle\omega_i(t)\rangle$, $\langle\mathbf{\Phi}_i(t)\rangle$, becomes necessary. This is equivalent to modelling the long-term development of the actual structure by an equivalent linear time-varying replacement with the circular frequencies $\langle\omega_i(t)\rangle$ and mode shapes $\langle\mathbf{\Phi}_i(t)\rangle$. Assuming that the structure is instrumented at $N$ points along the structure it will normally not be possible to determine more than the two lowest modes, i.e. the two lowest smoothed eigenfrequencies $\langle\omega_1(t)\rangle$, $\langle\omega_2(t)\rangle$ and the mode shape components $\langle\Phi_1^{(k)}(t)\rangle$, $\langle\Phi_2^{(k)}(t)\rangle$ of $\langle\mathbf{\Phi}_i(t)\rangle$ at the $k = 1,..,N$ measurement points. These smoothed modal quantities can be determined from the recorded acceleration time series by means of a multi input-multi output ARMAV-model, Kirkegaard et al. [3]. For convenience of notation, the identified modal parameters are collected in a measure vector $\mathbf{P}_M(t)$, ordered so $\mathbf{P}_M(t) = [\langle\omega_1(t)\rangle, \langle\omega_2(t)\rangle, \langle\Phi_1^{(1)}(t)\rangle, ..., \langle\Phi_1^{(N)}(t)\rangle, \langle\Phi_2^{(1)}(t)\rangle, ..., \langle\Phi_2^{(N)}(t)\rangle]$.

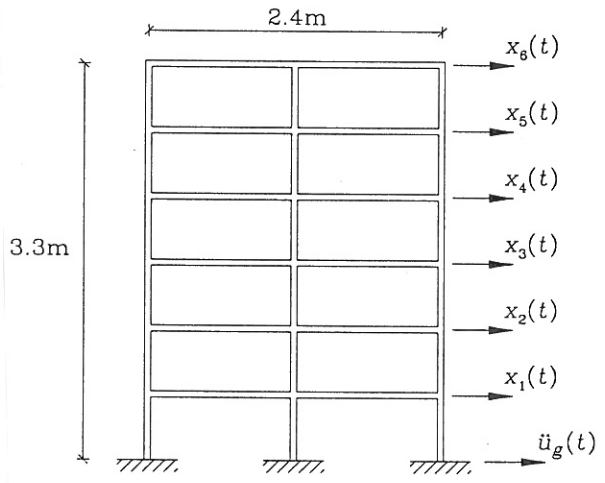


Figure 1: 2-bay, 6-storey model RC-frame.

Figure 2 shows computer simulated realizations of the 6 storey 2-bay structure shown in figure 1 subject to the horizontal base acceleration $\ddot{u}_g(t)$ and the horizontal storey displacements $x_i(t)$, $i = 1,..,6$ are the responses relative to the ground surface. In figure 3 the development in the two lowest cyclic eigenfrequencies are shown and in figures 4 and 5 the development in

the 1st and 2nd mode shapes at the six storeys are shown, respectively. In all the figures the smoothed values are shown as a solid line and the instantaneous values as a dotted line.

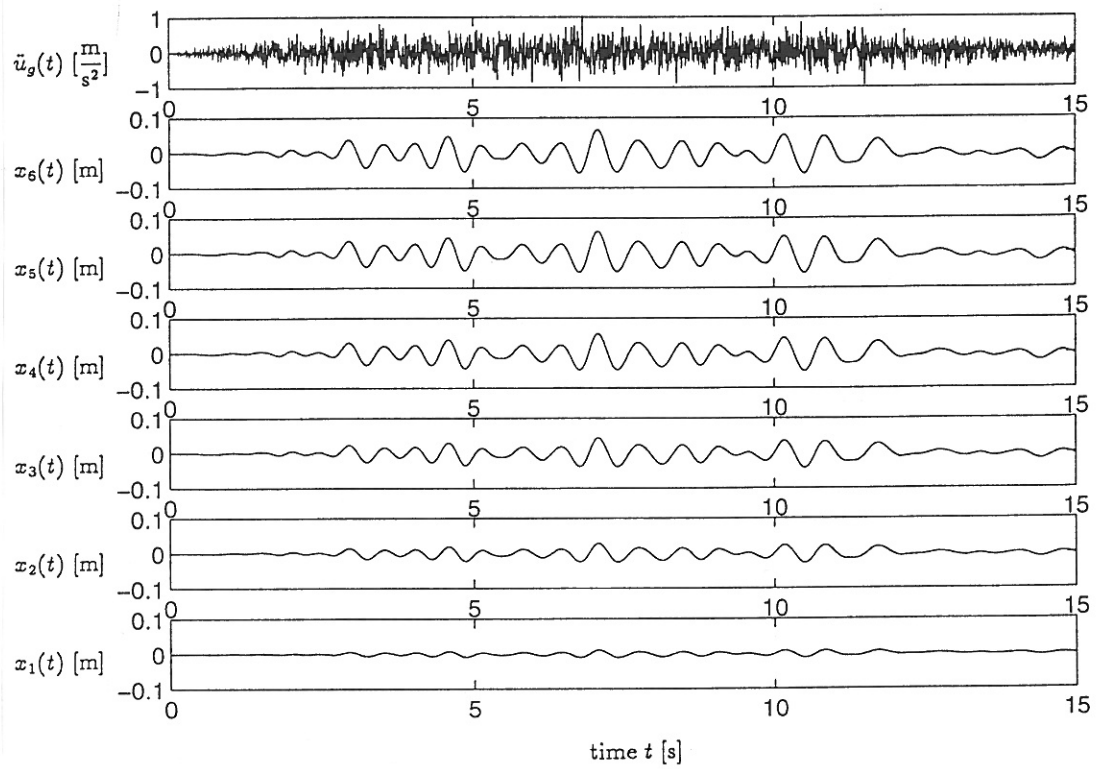


Figure 2: Ground surface acceleration time series and storey displacement time series. Simulation with SARCOF.

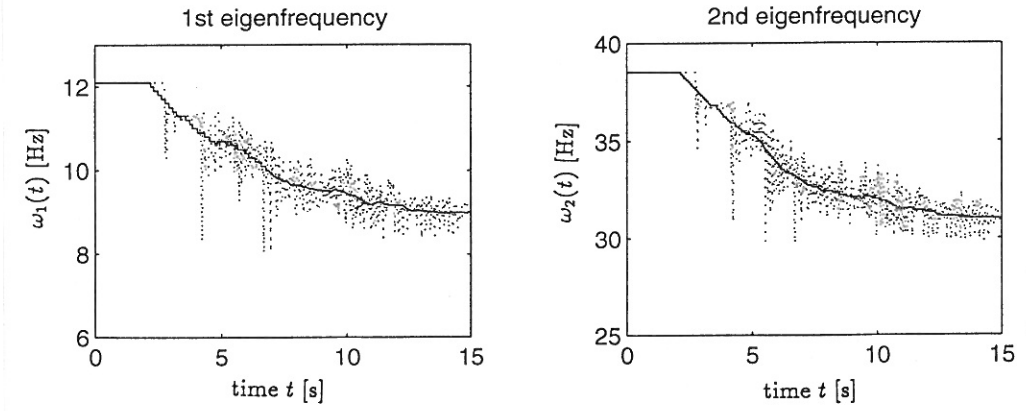


Figure 3: Development of the two lowest eigenfrequencies. [——]: Smoothed values, [· · ·]: instantaneous values. Simulation with SARCOF.

In the program, the smoothed values $\langle\omega_n(t_1)\rangle$ (or $\langle\Phi_n^{(k)}(t_1)\rangle$) at the time $t_1$ of the $n$th eigenfrequency have been evaluated by a moving window time average, Rodrigues-Gomes [6]

$$\langle\omega_n(t)\rangle = \frac{1}{T_a}\int_{t-\frac{T_a}{2}}^{t+\frac{T_a}{2}} \omega_n(\tau)d\tau \ , \quad T_a = 2.4\frac{2\pi}{\omega_1(0)} \tag{1}$$

where $T_a$ is the length of the averaging window.

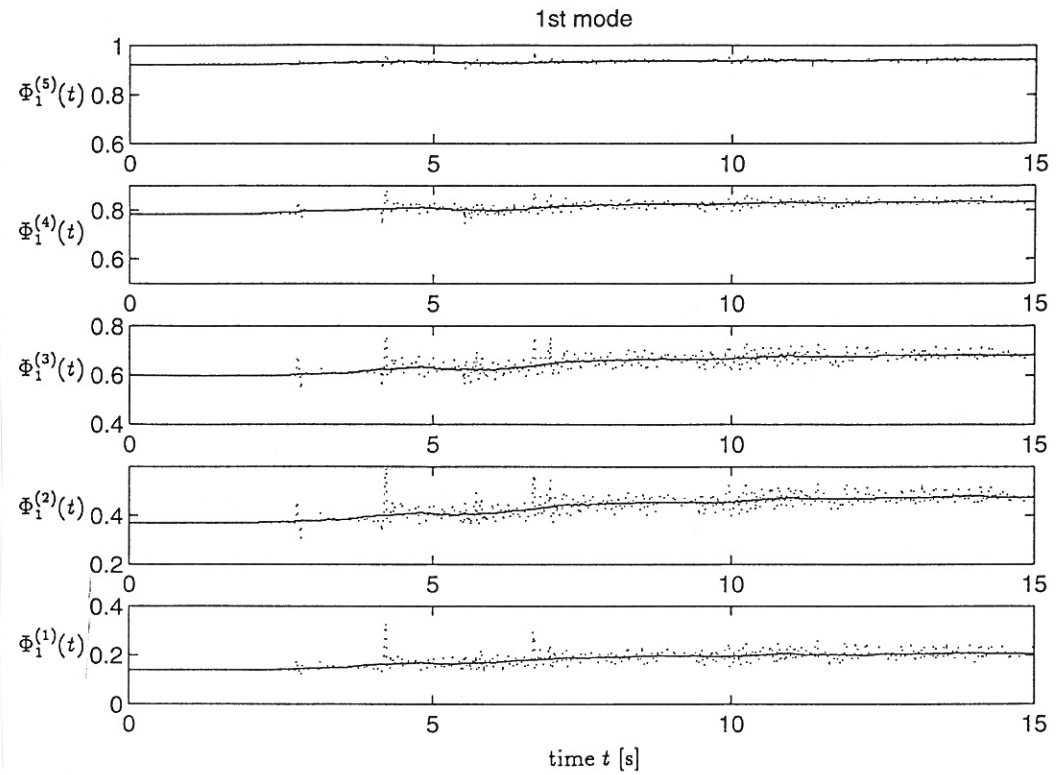


Figure 4: Development in the first mode shape. [——]: Smoothed values, [· · ·]: instantaneous values. Simulation with SARCOF.

The smoothed value of the fundamental frequency was used by DiPasquale et al. [1], [2] to define a global damage index $\delta_M$ called the maximum softening damage index. It is defined as the ratio between the undamaged fundamental eigenperiod $T_0$ and the maximum fundamental period $T_M = \max_{t\in[0,\infty[}\{T(t)\}$; of the softening system during a forced vibration event

$$\delta_M = 1 - \frac{T_0}{T_M} \tag{2}$$

The various local damage measures presented in this paper are extensions of this definition to the various substructures.

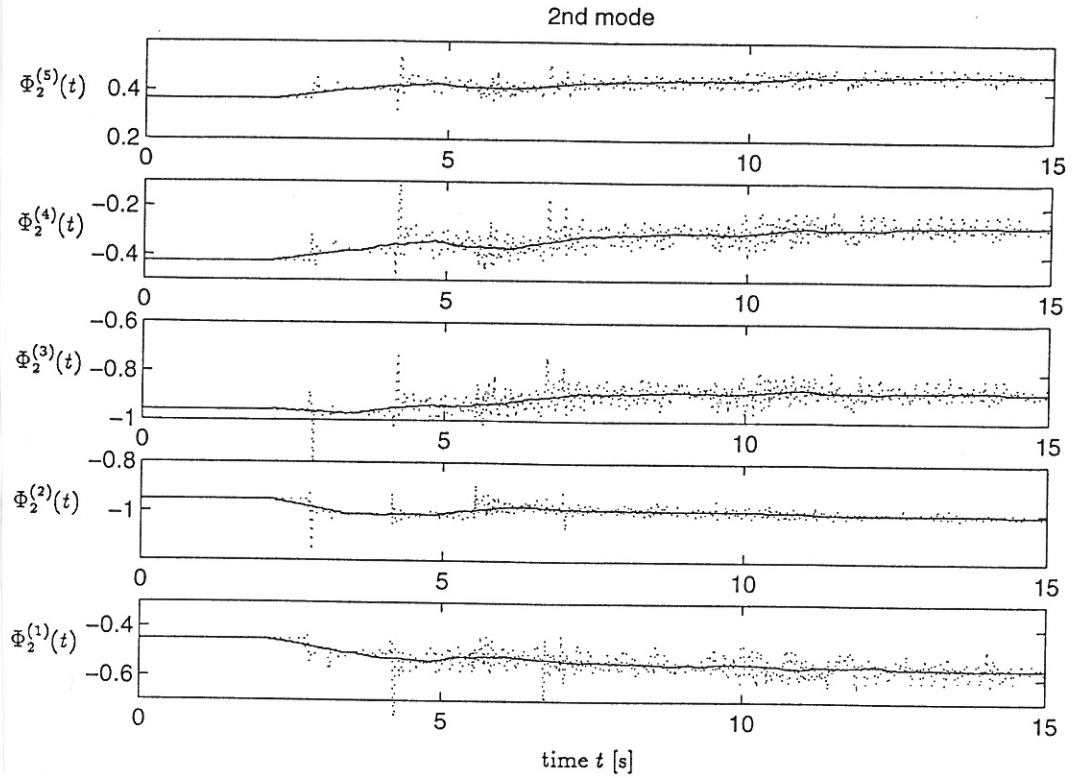


Figure 5: Development in the second mode shape. [——]: Smoothed values, [···]: instantaneous values. Simulation with SARCOF.

# 3 Description of Localization Procedure

The identification of the structural damage indices consists of two main phases:

1. Analysis of available records and estimation of modal parameters.
2. Evaluation of structural parameters by means of a substructure iteration with a least-square approach using the determined modal quantities from 1.

The main task in this paper is to investigate the second phase and the figures 3 and 4 can be considered as results of item 1 above. All investigations are based on simulated data, provided by the non-linear FEM program SARCOF (Stochastic Analysis Of Reinforced COncrete Frames). A detailed description of this program can be found in Mørk [4]. The proposed method for localization of damage is based on an earlier method developed by Skjærbæk et al. [7]. The main difference is that the present method is capable of using information from several response measurements along the structure.

In case of free vibrations where the structure remains in the linear elastic range, the motions are described by the following equation

$$\mathbf{M}\ddot{\mathbf{x}}(t) + \mathbf{K}_0\mathbf{x}(t) = \mathbf{0} \tag{3}$$

where $\mathbf{M}$ is the mass matrix and $\mathbf{K}_0$ is the undamaged stiffness matrix.

The corresponding modal quantities, eigenfrequencies $\omega_i$ and mode shapes $\mathbf{\Phi}_{i,0}$ of such a linear undamaged structure are determined from the eigenvalue problem

$$(\mathbf{K}_0 - \omega_{i,0}^2 \mathbf{M})\mathbf{\Phi}_{i,0} = \mathbf{0} \tag{4}$$

During a strong motion earthquake, the initial stiffness matrix $\mathbf{K}_0$ will start deteriorating causing changes in the modal parameters which are the parameters that can be "measured" through earthquake records. The task is therefore to solve this inverse problem of determining the time-varying elements in the stiffness matrix from the measured modal quantities. Normally this set of equations is underdetermined due to limited numbers of observations, and the limited number of modes activated, and therefore it requires special techniques to be solved.

The present damage localization is based on a sequence of sub-structurings in which the damage in each substructure is sequentially estimated. In the first iteration, the structure is divided into two substructures labelled 1 and 2 as illustrated in figure 6a, then

$$\mathbf{K}_0 = \mathbf{K}_{1,0}^{(1)} + \mathbf{K}_{2,0}^{(1)} \tag{5}$$

where $\mathbf{K}_{1,0}^{(1)}$ and $\mathbf{K}_{2,0}^{(1)}$ signify the global stiffness matrices of substructures 1 and 2. Although $\mathbf{K}_0$ is positive definite, its constituents $\mathbf{K}_{1,0}^{(1)}$ and $\mathbf{K}_{2,0}^{(1)}$ are both positive semi-definite, i.e. they contain a large number of zero components corresponding to the global positions of the extracted substructure. The subscripts 1 and 2 refer to substructures 1 and 2, and the subscript 0 refers to the initial state. The superscript (1) refers to the 1st time of substructuring.

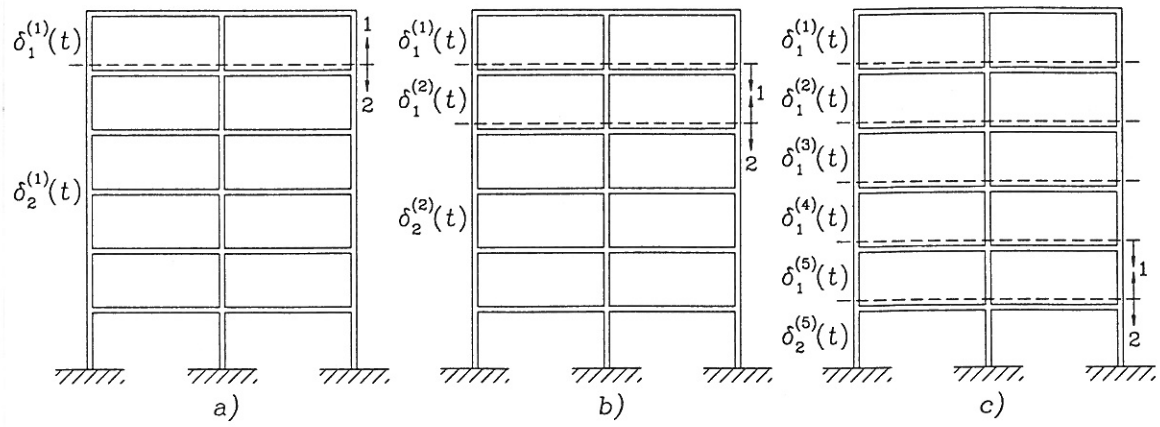


Figure 6: The procedure for changing the sequence of substructuring.

Next, a stiffness matrix $\mathbf{K}_e(t)$ for the equivalent linear structure can be defined in the following way.

$$\mathbf{K}_e^{(1)}(t) = \left(1 - \delta_1^{(1)}(t)\right)^2 \mathbf{K}_{1,0}^{(1)} + \left(1 - \delta_2^{(1)}(t)\right)^2 \mathbf{K}_{2,0}^{(1)} \tag{6}$$

$\delta_1^{(1)}(t)$ and $\delta_2^{(1)}(t)$ signify the damage indicators for substructures 1 and 2, respectively. These may be interpreted as measures of the averaged stiffness loss in the substructure. It should be noted here, that when only one substructure is used, the corresponding damage $\delta_1(t)$ measure is equivalent to the global softening obtained from eq. (2).

Next, $\delta_1^{(1)}$ and $\delta_2^{(1)}$ are identified, so $\mathbf{K}_e^{(1)}(t)$ as given by (6) provides the smoothed measured modal quantities $\mathbf{P}_M(t)$ identified from the available records, i.e.

$$\left(\sum_{j=1}^{2}\left(1-\delta_j^{(1)}(t)\right)^2\mathbf{K}_{j,0}^{(1)}-\langle\omega_i(t)\rangle^2\mathbf{M}\right)\langle\mathbf{\Phi}_i(t)\rangle=\mathbf{0} \tag{7}$$

where $\langle\mathbf{\Phi}_i(t)\rangle$ are the $i$th mode shape interpolated from the measured mode shape coordinates $\langle\Phi_i^{(k)}(t)\rangle$, $k=1,..N$. In case only one measurement along the structure is performed, the mode shapes cannot be interpolated and $\langle\mathbf{\Phi}_i(t)\rangle$ is replaced by $\mathbf{\Phi}_i$ which is the eigenvector to the matrix within the large parenthesis in (7) for a given set of damage indicators. How this is solved is explained in section 4.

The time-varying equivalent linear stiffness matrix of substructure 1 is then estimated as $\left(1-\delta_1^{(1)}(t)\right)^2\mathbf{K}_{1,0}^{(1)}$. Next, the previously labelled substructure 2 can be divided into two new substructures, again labelled 1 and 2. Then a new stiffness matrix of the equivalent linear structure can be written on the form

$$\mathbf{K}_e(t)=\left(1-\delta_1^{(1)}(t)\right)^2\mathbf{K}_{1,0}^{(1)}+\left(1-\delta_1^{(2)}(t)\right)^2\mathbf{K}_{1,0}^{(2)}+\left(1-\delta_2^{(2)}(t)\right)^2\mathbf{K}_{2,0}^{(2)} \tag{8}$$

where

$$\mathbf{K}_{2,0}^{(1)}=\mathbf{K}_{1,0}^{(2)}+\mathbf{K}_{2,0}^{(2)} \tag{9}$$

Since $\delta_1^{(1)}(t)$ is known, $\delta_1^{(2)}(t)$ and $\delta_2^{(2)}(t)$ can be estimated, inserting (8) into (7). From a new system identification, $\delta_1^{(2)}(t)$ and $\delta_2^{(2)}(t)$ are then obtained.
The procedure of dividing the previously labelled substructure 2 into 2 new substructures can be repeated further. Assuming that this procedure has been performed $i$ times, where eq. (6) corresponds to $i=1$ and eq. (8) to $i=2$. Then the stiffness matrix of the equivalent linear system can be written as.

$$\mathbf{K}_e^{(i)}(t)=\sum_{j=1}^{i-1}\left(1-\delta_1^{(j)}(t)\right)^2\mathbf{K}_{1,0}^{(j)}+\left(1-\delta_1^{(i)}(t)\right)^2\mathbf{K}_{1,0}^{(i)}+\left(1-\delta_2^{(i)}(t)\right)^2\mathbf{K}_{2,0}^{(i)} \tag{10}$$

In eq. (10) $\delta_1^{(1)}(t),.....,\delta_1^{(i-1)}(t)$ are known from previous identifications. $\delta_1^{(i)}(t)$ and $\delta_2^{(i)}(t)$ can be identified by inserting (10) into (7). Below, all the contributions to the stiffness from previous iterations, i.e. the summation $\sum_{j=1}^{i-1}\left(1-\delta_1^{(j)}(t)\right)^2\mathbf{K}_{1,0}^{(j)}$ will be referred to as $\mathbf{K}_{0,0}^{(i)}$ for convenience of notation.

By applying the above procedure, $\delta_1^{(i)}$ provides a measure of the average damage of each storey. If further localization within a given storey needs to be performed, it can in principle be done by fixing the damage at all other stories with the local damage indicators determined previously. The storey to be investigated can then be divided into two new substructures and new local damage indicators can be determined. When using the method it should be kept in mind that symmetrically placed elements in a symmetric structure will cause the same change in eigenfrequencies, and the localization is therefore limited to one of two possibilities.

# 4 Identification of Local Damage Indicators

The identification of the local damages $\delta_1^{(i)}(t)$ and $\delta_2^{(i)}(t)$ will be divided into two cases: $N = 1$ and $N > 1$ depending whether or not any mode shape component is measured.

In the first case the local damage indicators are identified in the following way. Initially, the eigenvalue problem (4) is solved by means of a subspace iteration yielding the two lowest eigenfrequencies $\omega_{1,0}$, $\omega_{2,0}$ and the corresponding mode shapes $\mathbf{\Phi}_{1,0}$ and $\mathbf{\Phi}_{2,0}$ of the undamaged structure.
A first estimate of the damage indicators at the time $t$ can be obtained using a Rayleigh fraction where the mode shapes of the undamaged structure are applied. Using the determined damage indicators $\delta_{1,1}^{(i)}$, $\delta_{2,1}^{(i)}$, new mode shapes can be determined as eigenvectors to $(\mathbf{K}_e(\delta_{1,1}^{(i)}, \delta_{2,1}^{(i)}) - \langle\omega_j(t)\rangle^2\mathbf{M})$. These new mode shapes are then used in the Rayleigh fraction and better local damage indicators are obtained. This procedure is repeated until a stable solution is found. The values of $\delta_1^{(i)}(t)$ and $\delta_2^{(i)}(t)$ at the $n$th step of this iteration process are designated $\delta_{1,n}^{(i)}(t)$, $\delta_{2,n}^{(i)}(t)$, respectively. The formulas at the $n$th iteration look as follows:

$$\langle\omega_j(t)\rangle^2 = \frac{\mathbf{\Phi}_{j,n-1}^T \mathbf{K}_e\left(\delta_{1,n}^{(i)}, \delta_{2,n}^{(i)}, t\right) \mathbf{\Phi}_{j,n-1}}{\mathbf{\Phi}_{j,n-1}^T \mathbf{M} \mathbf{\Phi}_{j,n-1}} \quad , \quad n = 1, 2, .... \tag{11}$$

where $\mathbf{\Phi}_{j,n-1} = \mathbf{\Phi}_{j,n-1}(t)$ are the mode shapes calculated at the $(n-1)$st step of iteration, i.e. corresponding to using the stiffness matrix $\mathbf{K}_e(\delta_{1,n-1}^{(i)}(t), \delta_{2,n-1}^{(i)}(t))$ in (7). Insertion of $\mathbf{K}_e(\delta_{1,n}^{(i)}(t), \delta_{2,n}^{(i)}(t))$ given by (10) into (11) provides the following two linear equations in $\left(1 - \delta_{1,n}^{(i)}(t)\right)^2$ and $\left(1 - \delta_{2,n}^{(i)}(t)\right)^2$ for the determination of the damage measures of $n$th iteration step.

$$\langle\omega_j(t)\rangle^2 = \frac{\mathbf{\Phi}_{j,n-1}^T \mathbf{K}_{1,0}^{(i)} \left(1 - \delta_{1,n}^{(i)}(t)\right)^2 \mathbf{\Phi}_{j,n-1} + \mathbf{\Phi}_{j,n-1}^T \mathbf{K}_{2,0}^{(i)} \left(1 - \delta_{2,n}^{(i)}(t)\right)^2 \mathbf{\Phi}_{j,n-1}}{\mathbf{\Phi}_{j,n-1}^T \mathbf{M} \mathbf{\Phi}_{j,n-1}}$$

$$+ \frac{\mathbf{\Phi}_{j,n-1}^T \mathbf{K}_{0,0}^{(i)} \mathbf{\Phi}_{j,n-1}}{\mathbf{\Phi}_{j,n-1}^T \mathbf{M} \mathbf{\Phi}_{j,n-1}}, \quad j = 1, 2 \tag{12}$$

From the determined values of the local damage indicators $\delta_{1,n}^{(i)}(t)$, $\delta_{2,n}^{(i)}(t)$, a new equivalent stiffness matrix can be calculated and new eigenmodes $\mathbf{\Phi}_{1,n}$, $\mathbf{\Phi}_{2,n}$ can be found from

$$\left(\mathbf{K}_e^{(i)}(\delta_{1,n}^{(i)}(t), \delta_{2,n}^{(i)}(t)) - \langle\omega_i(t)\rangle^2 \mathbf{M}_0\right) \mathbf{\Phi}_{i,n} = \mathbf{0} \tag{13}$$

This procedure eq. (11) to eq. (13) is repeated in each substructuring until no change occurs in the local damage indicator, i.e. $|\delta_{1,n}^{(i)} - \delta_{1,n-1}^{(i)}| + |\delta_{2,n}^{(i)} - \delta_{2,n-1}^{(i)}| < \epsilon$, where $\epsilon$ is a tolerance of the magnitude $10^{-5}$.

For the case where more than one measurement point along the structure are available (some components $\langle\Phi_i^{(k)}\rangle$ of the mode shapes $\langle\mathbf{\Phi}_i\rangle$ are estimated), the equations to be solved in each substructuring become overdetermined due to more known parameters than unknown. The solution in this case is found by means of a least square criterion.

Designating the measured modal parameters $\mathbf{P}_M(t)$ and the corresponding modal parameters of the structural model characterized by $\mathbf{M}$ and $\mathbf{K}_e(t)$ by $\mathbf{P}_S(t)$, an error vector $\mathbf{e}^{(i)}(t)$ can be defined as

$$e_j^{(i)}(\delta_1^{(i)}, \delta_2^{(i)}, t) = \frac{P_{M_j}(t) - P_{S_j}(\delta_1^{(i)}, \delta_2^{(i)}, t)}{P_{M_j}(t)}, \quad j = 1, 2, ... \tag{14}$$

A weighted mean-square-error can then be defined as

$$J^{(i)}(\delta_1^{(i)}, \delta_2^{(i)}, t) = \mathbf{e}^{(i)^T}\mathbf{W}\mathbf{e}^{(i)} = \sum_j W_{jj}(e_j^{(i)})^2 \tag{15}$$

where $\mathbf{W}$ is a positive definite weight matrix.

At each instant of time $t$ in the $i$th substructuring the local damage indicators $\delta_1^{(i)}(t), \delta_2^{(i)}(t)$ are determined in the following way:

1 Initially $\mathbf{P}_S^{(i)}(0,0,0)$ is determined for the undamaged structure by subspace iteration on (4).

2 The mean-square error $J^{(i)}(t)$ is calculated and a minimization with respect to the local damage indicators is performed. During the minimization $\mathbf{P}_S^{(i)}(\delta_1^{(i)}, \delta_2^{(i)}, t) = [\omega_1(t), \omega_2(t), \Phi_1^{(1)}, ..., \Phi_1^{(N)}, \Phi_2^{(1)}, ..., \Phi_2^{(N)}]$ is updated by solving

$$\left(\mathbf{K}_e^{(i)}(\delta_1^{(i)}(t), \delta_2^{(i)}(t)) - \omega_i(t)^2\mathbf{M}_0\right)\mathbf{\Phi}_i(t) = \mathbf{0} \tag{16}$$

3 The error vector $\mathbf{e}^{(i)}(\delta_1^{(i)}, \delta_2^{(i)}, t)$ and $J$ are calculated.

4 The steps 2-3 are repeated until $J$ reaches a minimum.

For both cases, it should be checked whether $(1 - \delta_j^{(i)(t)})^2$ becomes negative or larger than 1. If so, one the ajustments $(1 - \delta_j^{(i)})^2 = 0$ or $(1 - \delta_j^{(i)})^2 = 1$ are imposed, respectively.

# 5 Local Damage Indicators

Since in this study all data are artificially generated, it is possible to calculate damage indicators for each of the structural elements in the structure.

The element damage indicator used is based on the reduction of the average bending stiffness and is calculated directly by SARCOF, where a piecewise linear estimate of the slowly varying bending stiffness $EI(x,t)$ is obtained. An equivalent homogenous bending stiffness $\langle EI(t)\rangle$ in the element with the length $l$ can then be determined from averaging the flexibilities

$$\frac{l}{\langle EI(t)\rangle} = \int_0^l \frac{dx}{EI(x,t)} \tag{17}$$

Based on this averaged value of the bending stiffness, a local damage $\delta^k(t)$ of the element can be determined from

$$\langle EI(t)\rangle = (1 - \delta^k(t))^2 EI_0 \quad \Rightarrow \quad \delta^k(t) = 1 - \sqrt{\frac{\langle EI(t)\rangle}{EI_0}} \tag{18}$$

where $EI_0$ is the constant bending stiffness of the initially uncracked/cracked beam.

**Damage Index at Substructure Level**
Since the proposed method works at the substructure level which is not necessarily the same as the element level, it is necessary to be able to combine the element damage indices into one substructure damage index. This can be done using the dissipated hysteretic energy $E$ as weight, so

$$\delta^E_{substructure,i} = \sum_{j=1}^{q} \lambda_j \cdot \delta_j, \quad \lambda_j = \frac{E_j}{\sum_{k=1}^{q} E_i} \tag{19}$$

where $q$ is the number of elements in the $i$th substructure.

Alternatively, the weights could be the element damage indicator itself ($DI$) so the damage indicator of the substructure becomes

$$\delta^{DI}_{substructure,i} = \frac{\sum_{j=1}^{q} \delta_j^2}{\sum_{j=1}^{q} \delta_j} \tag{20}$$

This has e.g. been used by Park et al. [5].

# 6 Numerical examples

The structure considered is a 2-bay, 6-storey test-frame, scale 1:5. The modulus of elasticity of the reinforcement bars is $E = 2.1 \cdot 10^{11}$ Pa, the mass density of the concrete is $\rho_c = 2500\text{kg/m}^3$. All cross-sections are identical except for the reinforcements which are different in beams and columns. The parameters of the cross-sections are given in table 1. The two lowest circular eigenfrequencies of the cracked structure were calculated as $\omega_{1,0} = 12.1\text{s}^{-1}$, $\omega_{2,0} = 38.5\text{s}^{-1}$.

| | $A_s$ $[10^{-6}\text{m}^2]$ | $I$ $[10^{-6}\text{m}^4]$ | $E_c$ $[10^{10}\text{Pa}]$ |
|---|---|---|---|
| Beam | 5.65 | 0.41 | 3.5 |
| Column | 8.48 | 0.48 | 3.5 |

Table 1: *Characteristics of cross-sections.*

Two different load cases are considered. In the first case the structure is subjected to an earthquake generated by a Kanai-Tajimi filter exposed to a time-modulated white noise sequence with the following characteristics: duration $t_s = 15\text{s}$, circular peak frequency $\omega_0 = 10\text{s}^{-1}$, damping ratio $\zeta_0 = 0.3$ and time for maximum intensity $t_1 = 8\text{s}$. In the second case, the characteristics are: $\omega_0 = 35\text{s}^{-1}$, $\zeta_0 = 0.1$ corresponding to excitation in the second mode. In all cases the weights $W_{ii}$ are taken as 1 on eigenfrequencies and 0.1 on mode shape coordinates to assure that at least the correct magnitude of the damage is found.

**Excitation in the 1st mode**
Figures 3, 4 and 5 show the development in the circular eigenfrequencies and the normalized mode shapes as a function of time during the earthquake. The idea of the method is, as explained earlier, to use the smoothed eigenfrequencies which can be determined from one response measurement and one or more mode shapes determined from more measurements along the structure to estimate the average damage of selected substructures. The dependence of the

localization on the various inputs and measurements is investigated. The damage indicators are evaluated at the time $t_M$ of maximum softening in the first mode. In figure 7 the mode shapes of the initial and damaged structure at maximum softening are shown.

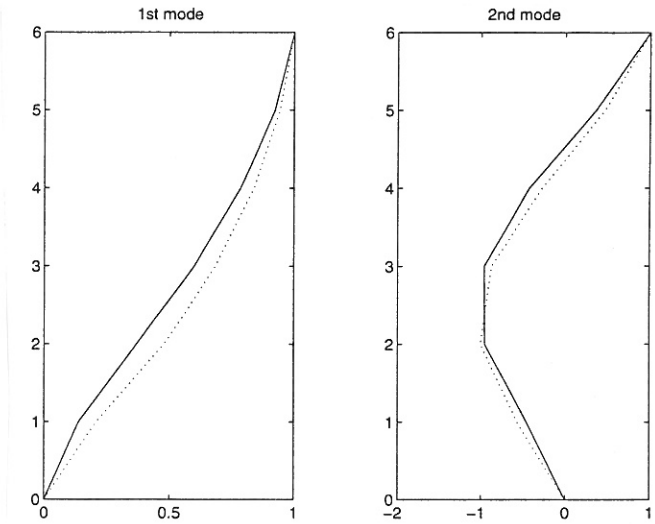


Figure 7: Mode shapes of the initial and damaged structure at maximum softening. Simulation with SARCOF. [——]: Undamaged, [· · ·]: Damaged.

The damage distribution is calculated with the proposed method for four different cases:

1. Only one measurement at the top storey is used: Only the two lowest frequencies are estimated from the response measurement.

2. The measurement at top-storey and one at another storey are used (5 combinations for a 6 storey frame).

3. The measurement at the top storey and at two other storeys are used (10 combinations for a 6 storey frame).

4. Measurement at all storeys.

For each of these cases the storey damage indicators are determined and compared to storey damage indicators determined by eq. (19) and eq. (20).
The results for these cases are shown in tables 2 and 3. The upper index of $\delta$ indicates at which storey/storeys measurements are performed. $\delta^0$ = only ground surface acceleration and top storey response are measured, $\delta^k$ = ground surface, $k$th storey ($k < 6$) and top storey are measured.

| Storey | $\delta^{k,E}_{substr.}$ | $\delta^{k,DI}_{substr.}$ | $\delta^0$ | $\delta^1$ | $\delta^2$ | $\delta^3$ | $\delta^4$ | $\delta^5$ |
|---|---|---|---|---|---|---|---|---|
| 1 | 0.36 | 0.36 | 0.27 | 0.37 | 0.25 | 0.30 | 0.27 | 0.23 |
| 2 | 0.24 | 0.35 | 0.39 | 0.39 | 0.47 | 0.39 | 0.38 | 0.37 |
| 3 | 0.06 | 0.16 | 0.23 | 0.03 | 0.08 | 0.17 | 0.25 | 0.33 |
| 4 | 0.00 | 0.03 | 0.00 | 0.00 | 0.00 | 0.00 | 0.00 | 0.00 |
| 5 | 0.00 | 0.00 | 0.00 | 0.00 | 0.00 | 0.00 | 0.00 | 0.00 |
| 6 | 0.00 | 0.00 | 0.00 | 0.00 | 0.00 | 0.00 | 0.00 | 0.00 |

Table 2: *Damage indicators at substructure (storey) level.*

| Storey | $\delta^{12}$ | $\delta^{13}$ | $\delta^{14}$ | $\delta^{15}$ | $\delta^{23}$ | $\delta^{24}$ | $\delta^{25}$ | $\delta^{34}$ | $\delta^{35}$ | $\delta^{45}$ | $\delta^{12345}$ |
|---|---|---|---|---|---|---|---|---|---|---|---|
| 1 | 0.36 | 0.36 | 0.36 | 0.24 | 0.29 | NC | 0.27 | 0.32 | 0.30 | 0.26 | 0.35 |
| 2 | 0.35 | 0.36 | 0.40 | 0.37 | 0.43 | | 0.46 | 0.40 | 0.39 | 0.38 | 0.36 |
| 3 | 0.10 | 0.08 | 0.00 | 0.32 | 0.07 | | 0.03 | 0.08 | 0.17 | 0.26 | 0.06 |
| 4 | 0.00 | 0.02 | 0.03 | 0.00 | 0.05 | | 0.08 | 0.04 | 0.00 | 0.00 | 0.05 |
| 5 | 0.00 | 0.00 | 0.00 | 0.00 | 0.00 | | 0.00 | 0.00 | 0.00 | 0.00 | 0.00 |
| 6 | 0.00 | 0.00 | 0.00 | 0.00 | 0.00 | | 0.00 | 0.00 | 0.00 | 0.00 | 0.00 |

Table 3: *Damage indicators at substructure (storey) level. NC: No convergence obtained.*

From table 2 it is clearly seen that in the case where one additional measurement is used, the best location is at the 1st floor if the highly damaged floors are to be precisely identified. On the other hand in this case the estimation of damage in the lightly damaged floors is poorer. In the case of two additional measuring points, it is seen that additional measurements at the 1st and 2nd storey provide a very good estimation of the damage.

**Excitation in the 2nd mode:**
The same calculations are performed for the case where the structure is excited in the second mode. The applied earthquake realization and corresponding storey displacements are shown in figure 8. Figures 9, 10 and 11 show the development in the cyclic eigenfrequencies and the normalized mode shapes as functions of time during the earthquake for the case where $\omega_0 = 35s^{-1}$, $\zeta_0 = 0.1$ obtained from the SARCOF program.

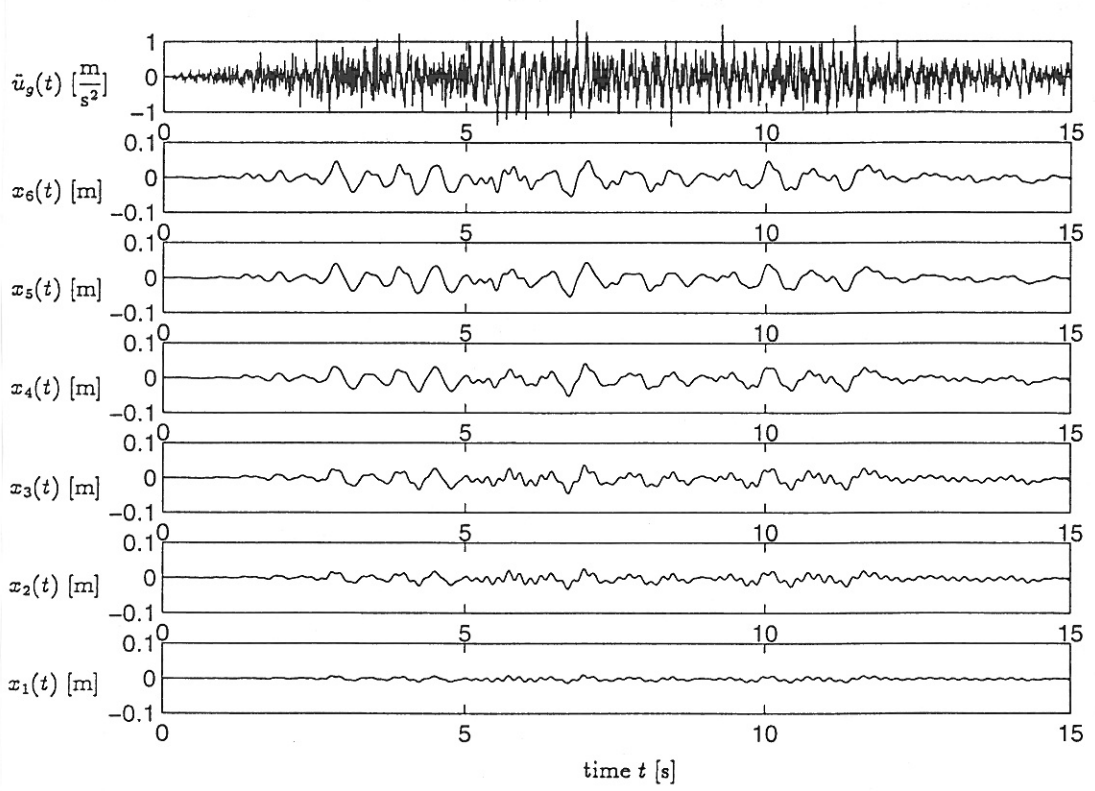


Figure 8: Ground surface acceleration time series and storey displacement time series. Simulation with SARCOF.

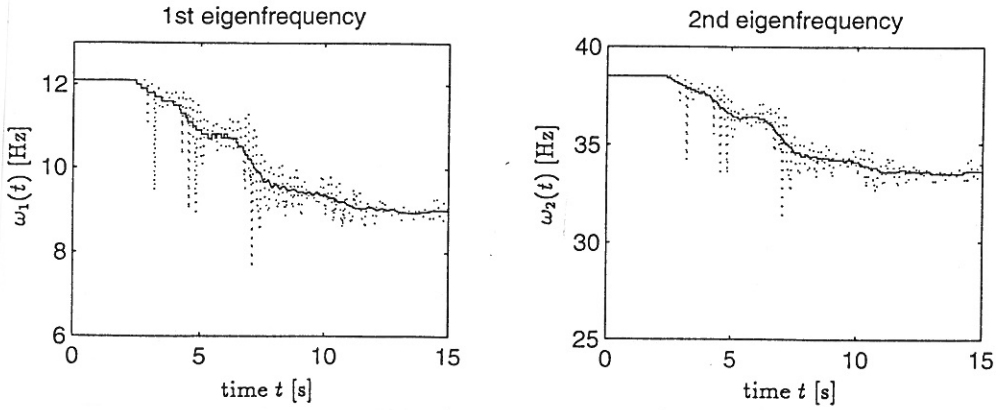


Figure 9: Development of the two lowest eigenfrequencies when excited in the 2nd mode. [——]: Smoothed values, [· · ·]: instantaneous values. Simulation with SARCOF.

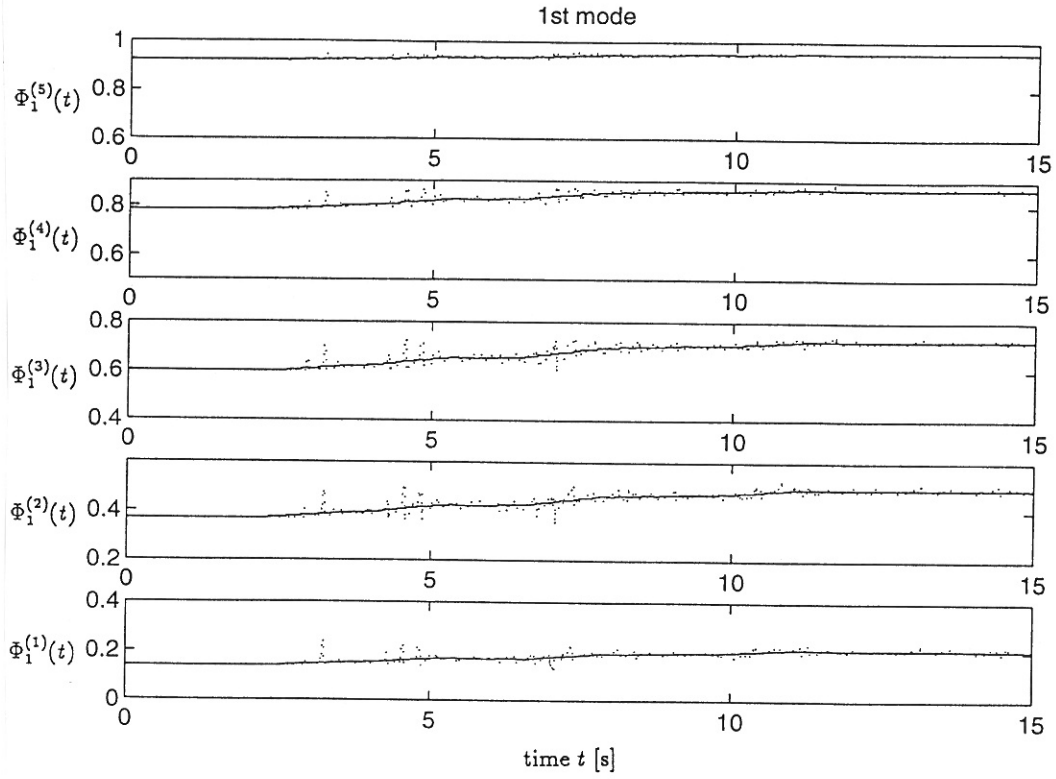


Figure 10: Development in the first mode shape when excited in the 2nd mode. [——]: Smoothed values, [· · ·]: instantaneous values. Simulation with SARCOF.

In figure 12 the mode shapes of the initial and damaged structure at maximum softening are shown.

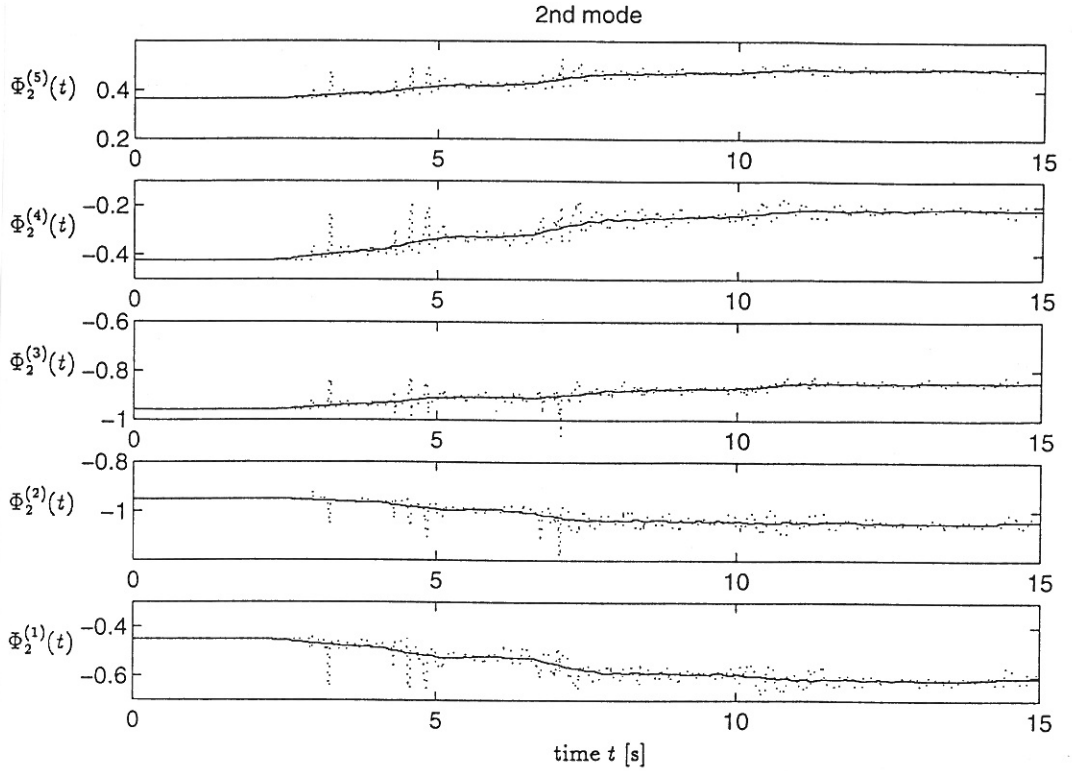


Figure 11: Development in the second mode shape when excited in the 2nd mode. [——]: Smoothed values, [· · ·]: instantaneous values. Simulation with SARCOF.

| Storey | $\delta^{k,E}_{substr.}$ | $\delta^{k,DI}_{substr.}$ | $\delta^0$ | $\delta^1$ | $\delta^2$ | $\delta^3$ | $\delta^4$ | $\delta^5$ |
|---|---|---|---|---|---|---|---|---|
| 1 | 0.38 | 0.40 | 0.38 | 0.38 | 0.38 | 0.26 | 0.40 | 0.07 |
| 2 | 0.19 | 0.29 | 0.19 | 0.33 | 0.25 | 0.22 | 0.28 | 0.40 |
| 3 | 0.03 | 0.12 | 0.25 | 0.01 | 0.22 | 0.45 | 0.10 | 0.22 |
| 4 | 0.06 | 0.19 | 0.18 | 0.13 | 0.03 | 0.00 | 0.00 | 0.38 |
| 5 | 0.09 | 0.13 | 0.01 | 0.12 | 0.12 | 0.05 | 0.15 | 0.00 |
| 6 | 0.02 | 0.08 | 0.00 | 0.06 | 0.17 | 0.34 | 0.15 | 0.10 |

Table 4: *Damage indicators at substructure (storey) level. Excitation in the 2nd mode.*

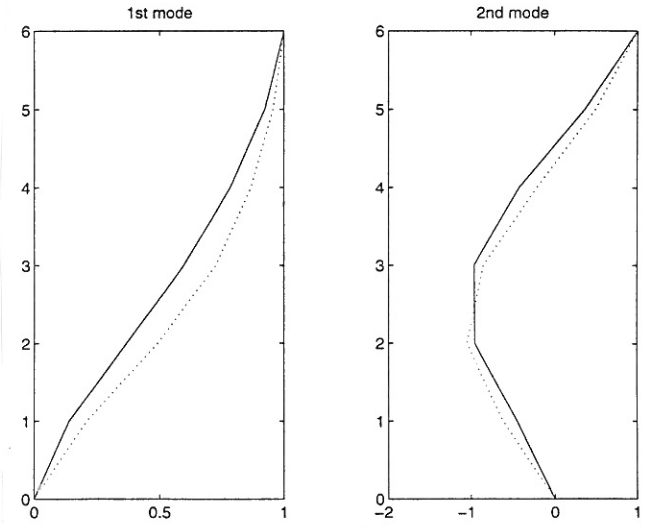


Figure 12: Mode shapes of the initial and damaged structure at maximum softening. Simulated with SARCOF. ——: Undamaged, [· · ·]: Damaged.

| Storey | $\delta^{12}$ | $\delta^{13}$ | $\delta^{14}$ | $\delta^{15}$ | $\delta^{23}$ | $\delta^{24}$ | $\delta^{25}$ | $\delta^{34}$ | $\delta^{35}$ | $\delta^{45}$ | $\delta^{12345}$ |
|---|---|---|---|---|---|---|---|---|---|---|---|
| 1 | 0.38 | 0.38 | 0.38 | 0.38 | 0.35 | NC | 0.35 | 0.29 | 0.33 | 0.36 | 0.37 |
| 2 | 0.27 | 0.30 | 0.33 | 0.31 | 0.31 | | 0.32 | 0.20 | 0.29 | 0.31 | 0.29 |
| 3 | 0.15 | 0.06 | 0.02 | 0.08 | 0.14 | | 0.13 | 0.45 | 0.25 | 0.10 | 0.08 |
| 4 | 0.06 | 0.19 | 0.11 | 0.07 | 0.17 | | 0.08 | 0.00 | 0.04 | 0.11 | 0.14 |
| 5 | 0.16 | 0.00 | 0.16 | 0.18 | 0.00 | | 0.20 | 0.03 | 0.21 | 0.15 | 0.13 |
| 6 | 0.10 | 0.19 | 0.00 | 0.04 | 0.23 | | 0.01 | 0.33 | 0.00 | 0.06 | 0.07 |

Table 5: *Damage indicators at substructure (storey) level. Excitation in the 2nd mode.*

In the case where the structure is excited in the 2nd mode it is seen that the damage is more spread out in the structure. In case of one additional measurement it is seen that if the highly damaged floors should be identified precisely the additional measurement should be performed at the 1st floor as in the first case. In case of two additional measurements it is seen that measurement at the 1st and 2nd or 1st and 3rd should be used.

In both of the considered cases it should be noted that even when only frequency information is used, the methods perform well and only have trouble in picking up the damage in the slightly damaged storeys.

# 7 Conclusions

The sensitivity of a method for localization and quantification of damage in members/substructures of structural systems is tested with respect to the information used. It is found that in the case where the structure is excited with frequencies close to the 1st mode the best localization and quantification of the damage is obtained if the top storey and one of the lower storey responses are measured. Only sligthly better performance is obtained if more measurements along the structure are used. For the case where the structure is excited with frequencies close to the second mode the same tendency is observed. As could be expected, it was found that the best localization is obtained if measurements at all storeys are used, but the improvement is negligible compared to the extra information that has to be collected. In comparing the various weighting procedures to combine the element damage indicators given by SARCOF into a substructure indicator the best match with the storey damage indicator obtained by the proposed method is obtained when the element damage indicator itself is used as the weighting factor. This is also to be expected since the damage indicator determined by the proposed method is only based on stiffness degradation which is not necessarily correlated to dissipated energy. The reason for this is that some elements are damaged simply by one big deformation while others are damaged by several low level cycles where much more energy is dissipated.

# 8 Acknowledgement

The present research was partially supported by The Danish Technical Research Council within the project: **Dynamics of Structures.**

# References

[1] DiPasquale, E. and Çakmak, A. Ş. *Detection of Seismic Structural Damage using Parameter-Based Global Damage Indices.* Probalistic Engineering Mechanics, Vol. 5, No. 2, pp. 60-65, 1990.

[2] DiPasquale, E. and Çakmak, A. Ş. *Seismic Damage Assessment using Linear Models.* Soil Dynamics and Earthquake Engineering, Vol. 9, No. 4, pp. 194-215, 1990.

[3] Kirkegaard, P.H., P. Andersen and R. Brincker, *Identification of the Skirt Piled Gullfaks C Gravity Platform using ARMAV Models.* Proceedings of the 14th IMAC, Dearborn, Michigan, USA, February 12-15, 1996.

[4] Mørk, K. J., *Stochastic Analysis of Reinforced Concrete Frames under Seismic Excitation.* Soil Dynamics and Earthquake Engineering, Vol. 11, No. 3, 1992.

[5] Park, Y.J., Wen, Y.K. and Ang, A. H.-S., *Two Dimensional Random Vibration of Hysteretic Structures.* Journal of Earthquake Engineering and Structural Dynamics, 1986, pp. 543-557.

[6] Rodriguez-Gomez, S., *Evaluation of Seismic Damage Indices for Reinforced Concrete Structures.* M.Sc. Thesis, Princeton University, Oct. 1990.

[7] Skjærbæk, P.S., Nielsen, S.R.K., Çakmak, A.S., *Assessment of Damage in Seismically Excited RC-structures from a Single Measured Response.* Proceedings of the 14th IMAC, Dearborn, Michigan, USA, February 12-15, 1996.

## FRACTURE AND DYNAMICS PAPERS

PAPER NO. 47: P. H. Kirkegaard & A. Rytter: *Use of Neural Networks for Damage Assessment in a Steel Mast.* ISSN 0902-7513 R9340.

PAPER NO. 48: R. Brincker, M. Demosthenous & G. C. Manos: *Estimation of the Coefficient of Restitution of Rocking Systems by the Random Decrement Technique.* ISSN 0902-7513 R9341.

PAPER NO. 49: L. Gansted: *Fatigue of Steel: Constant-Amplitude Load on CCT-Specimens.* ISSN 0902-7513 R9344.

PAPER NO. 50: P. H. Kirkegaard & A. Rytter: *Vibration Based Damage Assessment of a Cantilever using a Neural Network.* ISSN 0902-7513 R9345.

PAPER NO. 51: J. P. Ulfkjær, O. Hededal, I. B. Kroon & R. Brincker: *Simple Application of Fictitious Crack Model in Reinforced Concrete Beams.* ISSN 0902-7513 R9349.

PAPER NO. 52: J. P. Ulfkjær, O. Hededal, I. B. Kroon & R. Brincker: *Simple Application of Fictitious Crack Model in Reinforced Concrete Beams. Analysis and Experiments.* ISSN 0902-7513 R9350.

PAPER NO. 53: P. H. Kirkegaard & A. Rytter: *Vibration Based Damage Assessment of Civil Engineering Structures using Neural Networks.* ISSN 0902-7513 R9408.

PAPER NO. 54: L. Gansted, R. Brincker & L. Pilegaard Hansen: *The Fracture Mechanical Markov Chain Fatigue Model Compared with Empirical Data.* ISSN 0902-7513 R9431.

PAPER NO. 55: P. H. Kirkegaard, S. R. K. Nielsen & H. I. Hansen: *Identification of Non-Linear Structures using Recurrent Neural Networks.* ISSN 0902-7513 R9432.

PAPER NO. 56: R. Brincker, P. H. Kirkegaard, P. Andersen & M. E. Martinez: *Damage Detection in an Offshore Structure.* ISSN 0902-7513 R9434.

PAPER NO. 57: P. H. Kirkegaard, S. R. K. Nielsen & H. I. Hansen: *Structural Identification by Extended Kalman Filtering and a Recurrent Neural Network.* ISSN 0902-7513 R9433.

PAPER NO. 58: P. Andersen, R. Brincker, P. H. Kirkegaard: *On the Uncertainty of Identification of Civil Engineering Structures using ARMA Models.* ISSN 0902-7513 R9437.

PAPER NO. 59: P. H. Kirkegaard & A. Rytter: *A Comparative Study of Three Vibration Based Damage Assessment Techniques.* ISSN 0902-7513 R9435.

PAPER NO. 60: P. H. Kirkegaard, J. C. Asmussen, P. Andersen & R. Brincker: *An Experimental Study of an Offshore Platform.* ISSN 0902-7513 R9441.

PAPER NO. 61: R. Brincker, P. Andersen, P. H. Kirkegaard, J. P. Ulfkjær: *Damage Detection in Laboratory Concrete Beams.* ISSN 0902-7513 R9458.

PAPER NO. 62: R. Brincker, J. Simonsen, W. Hansen: *Some Aspects of Formation of Cracks in FRC with Main Reinforcement.* ISSN 0902-7513 R9506.

PAPER NO. 63: R. Brincker, J. P. Ulfkjær, P. Adamsen, L. Langvad, R. Toft: *Analytical Model for Hook Anchor Pull-out.* ISSN 0902-7513 R9511.

## FRACTURE AND DYNAMICS PAPERS

PAPER NO. 64: P. S. Skjærbæk, S. R. K. Nielsen, A. Ş. Çakmak: *Assessment of Damage in Seismically Excited RC-Structures from a Single Measured Response.* ISSN 1395-7953 R9528.

PAPER NO. 65: J. C. Asmussen, S. R. Ibrahim, R. Brincker: *Random Decrement and Regression Analysis of Traffic Responses of Bridges.* ISSN 1395-7953 R9529.

PAPER NO. 66: R. Brincker, P. Andersen, M. E. Martinez, F. Tallavó: *Modal Analysis of an Offshore Platform using Two Different ARMA Approaches.* ISSN 1395-7953 R9531.

PAPER NO. 67: J. C. Asmussen, R. Brincker: *Estimation of Frequency Response Functions by Random Decrement.* ISSN 1395-7953 R9532.

PAPER NO. 68: P. H. Kirkegaard, P. Andersen, R. Brincker: *Identification of an Equivalent Linear Model for a Non-Linear Time-Variant RC-Structure.* ISSN 1395-7953 R9533.

PAPER NO. 69: P. H. Kirkegaard, P. Andersen, R. Brincker: *Identification of the Skirt Piled Gullfaks C Gravity Platform using ARMAV Models.* ISSN 1395-7953 R9534.

PAPER NO. 70: P. H. Kirkegaard, P. Andersen, R. Brincker: *Identification of Civil Engineering Structures using Multivariate ARMAV and RARMAV Models.* ISSN 1395-7953 R9535.

PAPER NO. 71: P. Andersen, R. Brincker, P. H. Kirkegaard: *Theory of Covariance Equivalent ARMAV Models of Civil Engineering Structures.* ISSN 1395-7953 R9536.

PAPER NO. 72: S. R. Ibrahim, R. Brincker, J. C. Asmussen: *Modal Parameter Identification from Responses of General Unknown Random Inputs.*ISSN 1395-7953 R9544.

PAPER NO. 73: S. R. K. Nielsen, P. H. Kirkegaard: *Active Vibration Control of a Monopile Offshore Structure. Part One - Pilot Project.* ISSN 1395-7953 R9609.

PAPER NO. 74: J. P. Ulfkjær, L. Pilegaard Hansen, S. Qvist, S. H. Madsen: *Fracture Energy of Plain Concrete Beams at Different Rates of Loading.* ISSN 1395-7953 R9610.

PAPER NO 75: J. P. Ulfkjær, M. S. Henriksen, B. Aarup: *Experimental Investigation of the Fracture Behaviour of Reinforced Ultra High Strength Concrete.* ISSN 1395-7953 R9611.

PAPER NO. 76: J. C. Asmussen, P. Andersen: *Identification of EURO-SEIS Test Structure.* ISSN 1395-7953 R9612.

PAPER NO. 77: P. S. Skjærbæk, S. R. K. Nielsen, A. Ş. Çakmak: *Identification of Damage in RC-Structures from Earthquake Records - Optimal Location of Sensors.* ISSN 1395-7953 R9614.

**Department of Building Technology and Structural Engineering**
**Aalborg University, Sohngaardsholmsvej 57, DK 9000 Aalborg**
**Telephone: +45 98 15 85 22 Telefax: +45 98 14 82 43**